JOURNAL OF MODERN OPTICS, 15 OCTOBER 2004
VOL. 51, NO. 15, 2287–2295

Taylor & Francis
Taylor & Francis Group

Determining the orientation of the emissive dipole moment associated with dye molecules in microcavity structures

S. H. GARRETT, J. A. E. WASEY and W. L. BARNES

Thin Film Photonics Group, School of Physics, University of Exeter, Exeter EX4 4QL, UK; e-mail: S.H.Garrett@exeter.ac.uk

(*Received 19 February 2004*)

Abstract. We used cavity quantum electrodynamic effects to determine the orientation of a species of organic dye molecule located in a microcavity environment. We used the Langmuir–Blodgett technique to fabricate well-controlled multilayer structures into which we incorporated dye molecules with well-defined layer positions. Comparing the results of fluorescence lifetime measurements and radiation patterns with theoretical calculations allowed us to determine both the orientation and the quantum efficiency of the dye molecules.

1. Introduction

The fluorescence lifetime of an excited molecule is not a fixed property of the molecule; rather it depends on the local optical environment. In particular, the fluorescence lifetime and the spatial distribution of the emitted radiation can be modified by microcavity effects [1]. These effects have been extensively investigated and well documented [2]; they have been explored in the context of cavity quantum electrodynamics [3], as a means to improve the generation of light by light-emitting diodes [4] and may open the way to improve the quantum efficiency of weakly emitting species [5]. Here we use such effects to determine the orientation of the dipole moment associated with the emitter. Such information is important for many thin-film light-emitting devices, including organic light-emitting diodes (OLEDs) [6].

In a series of elegant experiments, Drexhage [7] showed how the fluorescence lifetime of Eu^{3+} ions changed as the distance between such ions and a highly reflective mirror was varied. These data were well accounted for by Chance *et al*. [8] who made use of a classical model in which the emitters were considered to be forced damped electric-dipole oscillators. Using a similar theory, we show in figure 1 (*a*) the results of theoretical calculations to indicate how the fluorescence lifetime varies as a function of the emitter–mirror separation for three different orientations of the dipole moment. Results for three different orientations of the dipole moment are considered; parallel, with the dipole moments lying in the plane of the film, perpendicular, and an isotropic distribution of dipole moment directions. For all three dipole orientations we see that the lifetime oscillates as the distance is increased. This can be understood as arising from interference between direct emission from the source, and a forcing term produced by the field reflected by the mirror that acts to drive the source [8]. When the emitter–mirror separation is such that the reflected field is in phase with the source, then emission is

Journal of Modern Optics ISSN 0950–0340 print/ISSN 1362–3044 online © 2004 Taylor & Francis Ltd
http://www.tandf.co.uk/journals
DOI: 10.1080/09500340410001703887

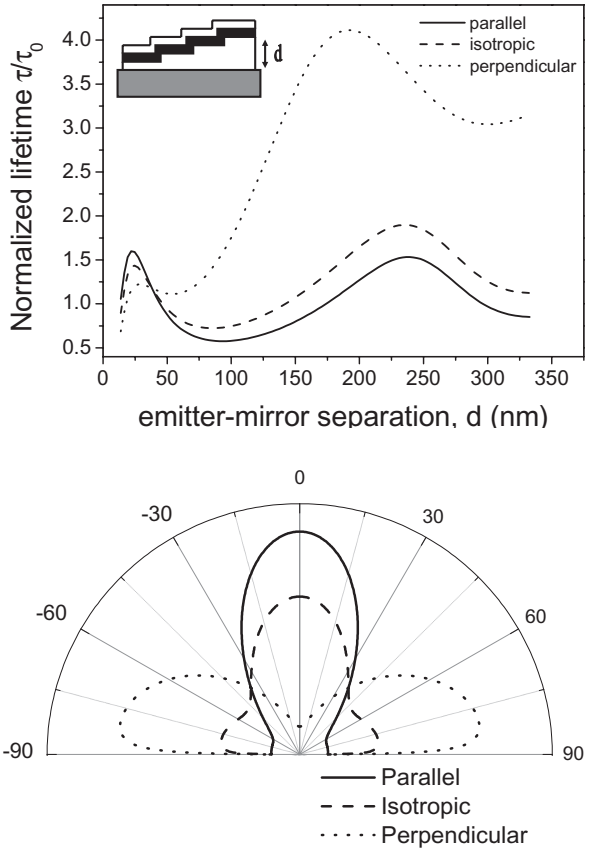

Figure 1. (*a*) The calculated normalized fluorescence lifetime for sources in front of a silver mirror shown as a function of fluorophore–mirror separation for three dipole orientations of the fluorophore; perpendicular to the mirror (...), parallel to the mirror (—), and an isotropic mixture of the two (- - - -). The emitters have an emission wavelength of 680 nm. The emission quantum efficiency is 1, the relative permittivities are $\varepsilon_{\mathrm{Ag}} = -19 + 1.2\mathrm{i}$ and $\varepsilon_{\mathrm{LB}} = 2.49$. The inset shows a schematic diagram of the sample geometry: R700-doped LB bilayer (grey) separated from an optically thick silver mirror (black) by a staircase of 22-tric LB layers (white). The theory plots account for a bilayer of 22-tric deposited on top of the dye layer in order to minimize bleaching effects. The normalization is with respect to emission from a source embedded in an infinite material of relative permittivity $\varepsilon_{\mathrm{LB}}$. (*b*) The calculated normalized polar emission patterns of four R700-doped LB layers separated from an optically thick silver mirror by 84 LB layers (i.e. approximately 235 nm) of 22-tric for three dipole orientations of the fluorophore; perpendicular to the mirror (...), parallel to the mirror (—), and an isotropic mixture of the two (- - - -). The emitted intensity is shown as a function of polar emission angle in degrees. Zero degrees is normal to the plane of the film.

enhanced and the lifetime is correspondingly reduced; when the reflected field is out of phase, the emission is suppressed and the lifetime is increased. Within a wavelength or so of the mirror, some of the emission takes place into surface plasmon modes rather than radiation and for very small separations the emission is further quenched by exciton excitation in the metal [9].

In addition to these effects on fluorescence lifetime, the radiation pattern is also altered. Importantly, the radiation pattern depends critically on the orientation of the emissive dipole moments. This is shown in figure 1 (*b*), from which we see the relevance of dipole orientation to light-emitting devices. In this work we specifically explore the role of dipole orientation in both fluorescence lifetimes and radiation patterns, by comparing experimental data with theoretical calculations.

The theoretically derived data presented in figure 1 (*a*) show that different dipole orientations result in strikingly different lifetime behaviour as the emitter–mirror separation is varied. In many fluorescing systems, including the Eu^{3+} ions used by Drexhage [7], the dipole moments are free to rotate randomly in space on a time scale much faster than the fluorescence lifetime; the dipole samples all spatial directions equally so that one can compute its lifetime τ_{ISO} by taking an appropriately weighted average $\tau_{ISO} = (1/3)\tau_{\perp} + (2/3)\tau_{\parallel}$, where $\tau_{\perp}$ and $\tau_{\parallel}$ are the lifetimes of dipoles oriented perpendicular and parallel respectively to the mirror. In other systems, for example the polymeric emissive materials used in some OLEDs, the dipole takes a well-defined direction. We see from figure 1 (*a*) that it should be possible to infer the dipole orientation from lifetime measurements. Such information is of value in OLED applications since the orientation of the dipole moment can have an important bearing on the efficiency of the device [10]. To explore this dipole orientation dependence on the fluorescence lifetime we investigated experimentally the lifetime modification of Rhodamine 700 (R700) molecules, a cyanine-type dye (supplied by Lambda Physik) with a broad emission band centred around 680 nm, in a variety of different microcavity geometries. The structure of the R700 molecule is shown in the inset of figure 2. To determine both the quantum efficiency and the dipole moment orientation, we compared the experimentally derived fluorescence data as a function of molecule–mirror separation with the theoretical predictions as shown in figures 1 (*a*) and (*b*).

It is important in such studies that good control is achieved over the positioning of the fluorescing molecules. They need to be placed at well-defined distances from the mirror, and this distance needs to be varied across the range of emitter–mirror separations of interest. Here we achieved this control by using the

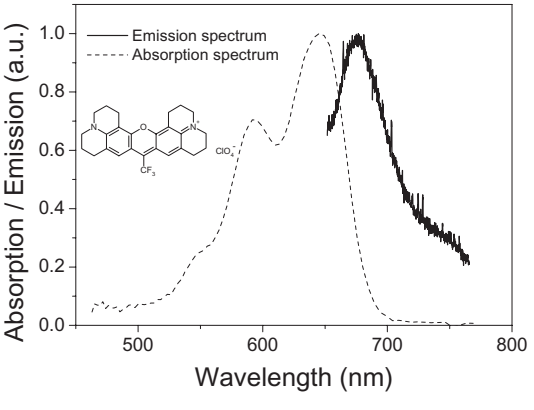

Figure 2. The absorption (- - - -) and emission (—) spectra of R700 (a.u., arbitrary units). The absorption maximum is around 650 nm, and the emission maximum around 680 nm. The inset shows the chemical structure of the R700 dye molecule.

Langmuir–Blodgett (LB) technique, as used in the original work of Drexhage [7]. This technique allows a thin organic film to be built up monolayer by monolayer. By introducing dye molecules into one or more of the monolayers, samples with which to probe the effect of the microcavity on the molecular fluorescence can be made.

2. Experimental details

Optically thick planar silver mirrors were formed by thermally evaporating silver on to polished $25\,\text{mm} \times 25\,\text{mm} \times 1\,\text{mm}$ fused silica substrates under a vacuum of 10^{-6} mbar. Before the silver surface of each sample was coated with LB layers it was rendered hydrophobic so as to ensure good Y-type deposition [11], accomplished by exposing the silvered substrate overnight to the vapour from several drops of 1,1,1,3,3,3-hexamethyldisilazane. With the silver film suitably treated, the next step was to add the LB layers needed to space the dye molecules from the mirror.

For the spacer layers, we used 22-tricosenoic acid (22-tric), a clear non-fluorescing LB film-forming molecule. Dye layers were deposited using 22-tric doped with R700. A doping concentration of R700 : 22-tric of 1 : 10 000 was chosen in order to ensure that the dye molecules were non-interacting. LB films of 22-tric doped with R700 at this level exhibited single-exponential fluorescence decays, higher concentrations showed non-exponential decay, possibly owing to dye molecule aggregation.

LB monolayers were compressed at a speed of $0.5\,\text{mm}\,\text{s}^{-1}$ prior to deposition. The deposition was performed at a surface pressure of $30\,\text{mN}\,\text{m}^{-1}$, this surface pressure being maintained by compressing the LB film as the monolayers were transferred to the substrate. As each of the monolayers was deposited, transfer ratios of around 1 were measured, indicating successful transfer of the film on to the substrate. Particular care was taken to ensure good deposition of the first bilayer of any given LB multilayer by using a low speed of monolayer transfer to the substrate, typically $0.15\,\text{mm}\,\text{s}^{-1}$ on the downstroke and $0.10\,\text{mm}^{-1}\text{s}^{-1}$ on the upstroke. The combination of slow deposition speeds and the hydrophobic treatment of the surface ensured that no wetting of the silver occurred. Once the first bilayer had been transferred successfully, the dipping speed was increased to $0.30\,\text{mm}\,\text{s}^{-1}$ for the downstrokes, and $0.25\,\text{mm}\,\text{s}^{-1}$ for the upstrokes. The 22-tric spacer layers for a given sample were deposited in one session, after which the sample was left in a desiccator for at least 24 h to allow any residual surface water to evaporate. When not in use for measurements, samples were stored in a desiccator, in a light-tight environment.

The optical properties of the R700 were characterized by depositing R700-doped 22-tric LB films on to a polished silica substrate. The absorption spectrum was measured by recording transmittance as a function of illumination wavelength. The emission spectrum was obtained by pumping the sample with a red He–Ne laser (wavelength of 632.8 nm, coincident with the R700 absorption spectrum) and collecting the fluorescence as a function of wavelength. The absorption and emission spectra are shown in figure 2.

To obtain fluorescence lifetime measurements the R700 molecules were pumped at 635 nm by a pulsed diode laser with a pulse width less than 50 ps full width at half-maximum, and a repetition rate of 1 MHz. Fluorescence was

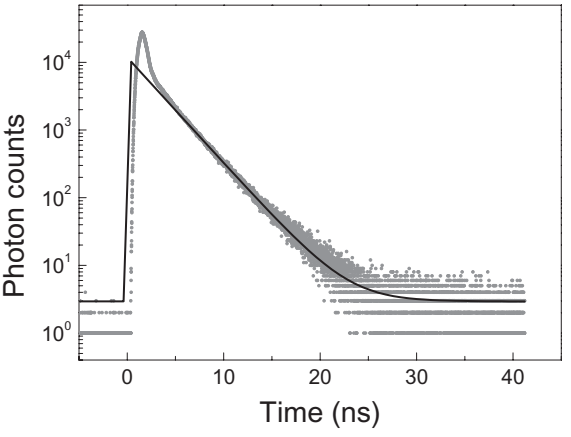

Figure 3. A typical example of the time-resolved fluorescence data. A single-exponential function of the form $I(t) = I_B + I_0 e^{-t/\tau}$ has been fitted to the data in the region 8.5 ns $\leq t \leq$ 41 ns, giving a lifetime of 2.85 ± 0.05 ns.

collected with a lens, filtered by 648 nm long-pass filters in order to cut out most of the pump light, and detected by a photodetector using a time-correlated single-photon counting module (Jobin Yvon IBH Ltd). In order to obtain enough counts to fit the lifetime with good statistical accuracy, data were acquired until a peak height of at least 10^4 counts was reached. Background counts of 0–2 photons per pump pulse were typical.

A typical example of the fluorescence decay data is shown in figure 3. A single-exponential function of the form $I(t) = I_B + I_0 \exp(-t/\tau)$ has been fitted to the data. The initial peak, centred at $t = 1.5$ ns, is due to residual scattered pump light; the extent of these unwanted data was ascertained by taking measurements from a control sample that was identical except that it contained no R700 dye molecules. The control sample yielded negligible counts beyond $t = 8.5$ ns, consequently we fitted a single-exponential decay to the data in the 8.5–41.0 ns interval.

3. Results

The spacer layer sample geometry (inset of figure 4) was fabricated via the LB technique, and the R700 fluorescence lifetime was measured as described above. The data are shown in figure 4, together with the best theoretical fits obtained for the three different dipole orientations. It is immediately clear that some information about the dipole orientation can be inferred; the lifetime data cannot be accounted for by a perpendicular dipole orientation. The choice between parallel and isotropic dipole orientations is less clear, there is little to choose between the two theoretical fits. For this reason, we sought an alternative microcavity geometry, one that might offer better discrimination between these possibilities.

There are several variables that can be adjusted in the model in order to achieve a fit to the data. As well as the thickness of the individual LB layers, which we found to be 2.75 nm, the distance dependence of the lifetime also depends on the quantum efficiency of emission from the dye molecules [12]. By fitting theory to our data we find that the quantum efficiency of R700 in an LB environment can be accurately deduced from the amplitude of the lifetime oscillation in the spacer

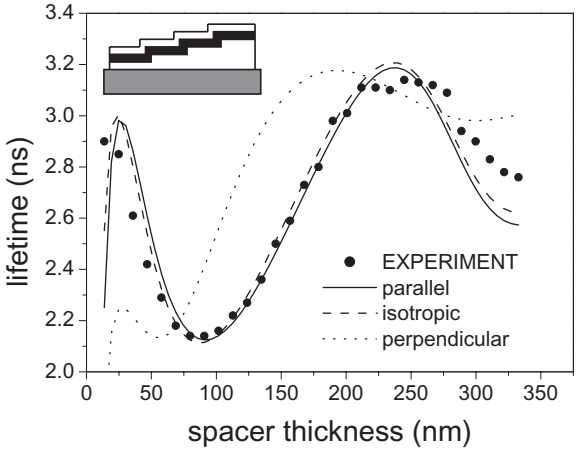

Figure 4. The measured lifetimes of R700 molecules in an LB environment in front of a silver mirror are shown as a function of emitter–mirror separation. The theoretical curve for the perpendicular dipole moment orientation does not fit the data, although it is difficult to choose between the parallel and isotropic theoretical fits for these data. The quantum efficiency used for the parallel fit is 0.4; the free-space fluorescence lifetime is 2.75 ns. The quantum efficiency used for the perpendicular fit is 0.49, the free-space fluorescence lifetime is 2.0 ns. The quantum efficiency used for the isotropic fit is 0.48, the free-space fluorescence lifetime is 2.48 ns. $\varepsilon_{\mathrm{Ag}} = -18 + 2\mathrm{i}$ for all fits. The rather high value of the imaginary component may arise because scattering losses produced by the LB film are accounted for in this parameter; scattering losses could not be directly incorporated into the calculation. The inset shows a schematic diagram of an R700-doped LB bilayer (grey) separated from an optically thick silver mirror (black) by a staircase of 22-tric LB layers (white). A bilayer of 22-tric was deposited on to the dye layer in order to minimize bleaching effects.

layer geometry (figure 4) to be $q = 0.4 \pm 0.05$. This value for the quantum efficiency was used in the fitting of theory to the experimental data for subsequent sample geometries. However, as noted above, from the results of this sample geometry (figure 4), one cannot discriminate between the case when the dipole moments are parallel or when they are in an isotropic distribution. The forms of the two distributions are very similar, and they both show the main features evident in the experimental data.

4. Overlayer sample geometry

In order to resolve the question of the dipole orientation we examined an alternative sample geometry, one in which the emitter–mirror separation was fixed, but an increasing number of 22-tric layers were added on top of the dye-doped layers. Theoretical modelling indicated that this structure might allow us to differentiate between parallel and isotropic orientations. To explore this second sample geometry, which we call the overlayer geometry, a R700 film was deposited at a fixed distance from the silver mirror, and the number of 22-tric overlayers was increased (see inset of figure 5). The sample was pumped in the same way as for the spacer layer geometry described in the previous section, and the fluorescence lifetimes determined in the same way.

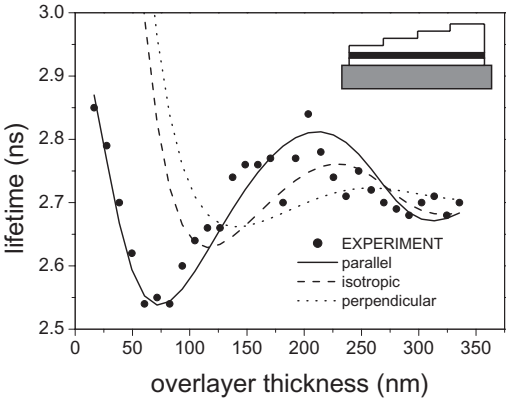

Figure 5. The measured lifetimes of R700 molecules in an LB environment in front of a silver mirror are shown as a function of emitter–air–22-tric interface separation. The theoretical curve for isotropic dipole moment orientation does not fit the data, leaving us to conclude that the dipole moments lie parallel to the plane of the LB film. The quantum efficiency used for the parallel fit is 0.4, the free-space fluorescence lifetime is 2.73 ns. The quantum efficiency used for the perpendicular fit is 0.2; the free-space fluorescence lifetime is 4.7 ns. The quantum efficiency used for the isotropic fit is 0.48 the free-space fluorescence lifetime is 4.32 ns. $\varepsilon_{\mathrm{Ag}} = -18 + 2\mathrm{i}$ for all fits. The inset shows a schematic diagram of an R700-doped LB layer (grey) separated from an optically thick silver mirror (black) by six LB layers of 22-tric (white), with a staircase of 22-tric LB layers (white) deposited on top of the R700.

We again compared the experimental data from the overlayer samples with theoretical data based on parallel, perpendicular and isotropic orientations (figure 5). The comparison between experiment and theory for this geometry shows that an isotropic distribution of dipole moments does not satisfactorily fit the experimental results, whilst the parallel distribution gives a much better account. We conclude that the R700 dipole moments lie in the plane of an LB film. Using weighted combinations of isotropic and parallel dipole orientations to fit the data, we found that the best fit comes from using the assumption of only parallel dipole moments.

As shown in figure 1 (*b*), an emitting dipole will produce a radiation pattern that depends on the orientation of the dipole moment of the emitter. A large ensemble of emitters having a well-defined orientation of their dipole moments can thus be expected to emit light with a characteristic and well-defined spatial distribution. With this in mind, our next sample geometry was fabricated in order to use the measurement of the spatial distribution of emission to infer the dipole moment orientation of the emitters. The sample geometry used for this is shown in the inset of figure 6. We chose this sample geometry because theoretical predictions suggested that such a sample would possess one of three distinct radiation patterns, depending on whether the dipole moment orientation of the emitters was isotropic, parallel or perpendicular to the plane of the dye-doped film.

5. Radiation patterns

Radiation patterns for a microcavity structure were measured (figure 6). Emission intensity data are plotted as a function of angle relative to the normal

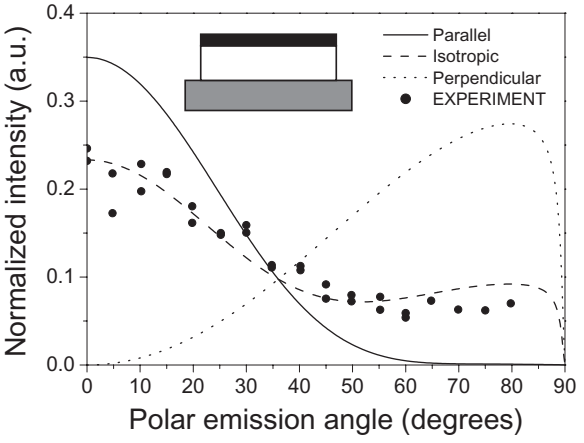

Figure 6. The measured radiation intensity of R700 molecules in an LB environment in front of a silver mirror is shown as a function of angle relative to the surface normal (a.u., arbitrary units). The theoretical curves for horizontal or vertical dipole moment orientation do not fit the data, leaving us to conclude that the dipole moments are in an isotropic distribution in the film, or at least a proportion of the dipole moments do not lie horizontally. The inset shows a schematic diagram of four R700-doped LB layers (grey) separated from an optically thick silver mirror (black) by 84 LB layers of 22-tric (white).

to the film, account being taken of the bleaching of the dye molecules. The best theoretical fits to the data are plotted on the same axes. The experimental measurements were problematic owing to the low intensity of emission. Unfortunately the greatest difference in radiation patterns for the different dipole moment orientations was found to occur for thicknesses of this sample geometry that exhibit a relatively low emission intensity. This in turn led us to use a doping concentration of R700 : 22-tric of 1 : 100, instead of the 1 : 10 000 used for the lifetime measurements, in order to collect enough emission to plot a radiation pattern. The sample was pumped with a 410 nm continuous-wave laser for this measurement rather than the 633 nm He–Ne laser used for the lifetime measurements; this was necessary in order to have a large spectral separation between the pump and the dye emission. The sample was mounted on a rotating stage, and the emitted fluorescence was focused into a stationary charge-coupled device camera. The results plotted in figure 6 are inconclusive, but the best theoretical fits to the data for each orientation considered suggest an isotropic distribution of dipole moment directions, or at least a proportion of non-parallel dipoles. Since the isotropic theoretical fits are based on a one-third to two-thirds mix of the theoretical fits for perpendicular and parallel dipole moments, it is quite possible that the best fit to these radiation pattern data is achieved by having different weightings of perpendicular and parallel dipole moments in the calculation. However, it is clear from the three theoretical fits to the data shown in figure 6 that this radiation pattern is not due to a purely parallel dipole moment orientation. This is in contrast with the inference from the fluorescence lifetime data in figure 5. This may be due to the high doping concentration of R700 used for this study. We postulate that one can introduce a low number concentration of dopants into a 22-tric LB film and the dopants can align into a well-defined orientation,

in this case parallel to the plane of the film, but that, when the concentration of dopants is much higher, in this case 100 times higher, the LB film is disrupted by the dopants, and the previously well-defined dipole moment orientation is lost. Further work is needed to investigate this issue.

6. Summary

In this paper we have presented fitted fluorescence lifetimes for several sample geometries to demonstrate the dependence of lifetime modification on dipole orientation and have found from our measurements that the orientation of the dipole moments associated with R700-doped 22-tric LB films are principally in the plane of the film.

We have identified two geometries of microcavity suitable for dipole orientation determination via lifetime measurements that could be of value for emissive materials pertinent to light-emitting devices. The samples used for lifetime measurements consist of staircases of 22-tric LB layers deposited on to the silver mirror; dye is doped into layers on the top of the staircase or at a fixed separation from the mirror, with the staircase structure on top. We have also measured the radiation pattern of a highly doped dye layer in an LB microcavity environment; we found that the theoretical fits to the experimental data suggest an isotropic dipole moment orientation, rather than the parallel dipole moment orientation suggested by the fluorescence lifetime data. Future work will address this issue which we suspect arises from the high doping concentration necessary to make these measurements.

Acknowledgment

The authors would like to thank the Engineering and Physical Sciences Research Council for partially funding this work.

References

[1] Ford, G. W., and Weber, M. G., 1984, *Phys. Rep.*, **113,** 197.
[2] Amos, R., and Barnes, W. L., 1997, *Phys. Rev.* B, **55,** 7249.
[3] Berman, P. R., 1994, *Cavity Quantum Electrodynamics* (New York: Academic Press).
[4] Benisty, H., De Neve, H., and Weisbuch, C., 1998, *J. Quant. Electron.*, **34,** 1612.
[5] Lakowicz, J. R., 2001, *Anal. Biochem.*, **298,** 1.
[6] Cimrová, V., and Neher, D., 1996, *J. Appl. Phys.*, **79,** 3299.
[7] Drexhage, K. H., 1970, *Scient. Am.*, **222,** 108.
[8] Chance, R. R., Prock, A., and Silbey, R., 1978, *Adv. Chem. Phys.*, **37,** 1.
[9] Barnes, W. L., 1998, *J. Mod. Optics*, **45,** 661.
[10] Smith, L. H., Wasey, J. A. E., Barnes, W. L., 2004, *Appl. Phys. Lett.*, **84,** 2986.
[11] Andrew, P., 1998, PhD Thesis, University of Exeter.
[12] Astilean, S., and Barnes, W. L., 2002, *Appl. Phys.* B, **75,** 591.